

A Two-Step Method for Energy-Efficient Train Operation, Timetabling and On-Board Energy Storage Device Management

Chaoxian Wu, Shaofeng Lu*, Fei Xue, Lin Jiang, Minwu Chen and Jie Yang

Abstract—This paper proposes a novel two-step approach to concurrently optimize the train operation, timetable and energy management strategy of the on-board energy storage device (OESD) to minimize the net energy consumption for a whole urban railway line. In Step 1, approximating functions representing the minimum net energy consumption of each specific inter-station operation is obtained by data fitting based on the previous research outcomes. In Step 2, the optimal running time, initial state of energy (ISOE) of OESD, train speed profiles, discharge/charge management of the OESD during each inter-station journey and at each station are obtained by applying convex optimization formulated by approximating functions gained in Step 1. The method is firstly tested with several general train cases to show its robustness and adaptability. Then a real-world case based on Beijing metro Yizhuang line is studied and the optimal solution is found to reduce the net energy consumption 1.04%, 2.09% and 23.77% for a service cycle of a single train when compared to other operation scenarios, i.e. Fully Charged, No Management and No OESD scenario, respectively. The approach is also computationally efficient with a computational time less than 1 min, namely 38.86 s for the upline and 48.38 s for the downline, spent on finding the optimal solution.

Index Terms—Train operation, timetable, on-board energy storage device (OESD), energy management, data fitting, convex

This research project is supported and sponsored in part by National Natural Science Foundation of China under Grant 61603306, Grant 51877181, Grant 51877182 and Grant 62063009 and in part by the Research Development Fund RDF-16-01-42 at Xi'an Jiaotong-Liverpool University and in part by the Fundamental Research Funds for the Central Universities NO. 2020ZYGXZR087 and in part by State Key Laboratory of Rail Traffic Control and Safety (Contract No. RCS2021K008), Beijing Jiaotong University).

Chaoxian Wu is with the Shien-Ming Wu School of Intelligent Engineering, South China University of Technology, China, the Department of Electrical Engineering and Electronics, University of Liverpool, UK and the Department of Electrical and Electronic Engineering, Xi'an Jiaotong-Liverpool University, China (Email: Chaoxian.Wu@liverpool.ac.uk)

Shaofeng Lu is with the Shien-Ming Wu School of Intelligent Engineering, South China University of Technology, China (Email: lushaofeng@scut.edu.cn)

Fei Xue is with the Department of Electrical and Electronic Engineering, Xi'an Jiaotong-Liverpool University, China, 215123; (Email: Fei.Xue@xjtlu.edu.cn)

Lin Jiang is with the Department of Electrical Engineering and Electronics, University of Liverpool, Liverpool L69 3GJ, U.K. (Email: ljjiang@liverpool.ac.uk)

Minwu Chen is with National Rail Transportation Electrification and Automation Engineering Technology Research Center, Chengdu 610031, China and also with the School of Electrical Engineering, Southwest Jiaotong University, Chengdu 610031, China (Email: chenminwu@home.swjtu.edu.cn)

Jie Yang is currently a professor and the director with Jiangxi Key Laboratory of Maglev Technology (JKLMT) and the Institute of Permanent Maglev and Railway Technology (IPMRT) at Jiangxi University of Science and Technology, Ganzhou, China; (Email: 15405993@qq.com)

*Corresponding Author: Dr. Shaofeng Lu, Shien-Ming Wu School of Intelligent Engineering, South China University of Technology, China. Phone: +86(0)20-8118-2116. (Email: lushaofeng@scut.edu.cn),

optimization

I. INTRODUCTION

With the rapid development of railway electrification, intelligent energy management is indispensable for saving the energy consumed by increasing travel demand [1]. To improve the energy efficiency of the railway systems, train operation and timetabling optimization are two popular approaches to help reduce the energy consumption without changing the existing infrastructures [2], [3]. On the other hand, in rail industry the regenerative energy has been utilized and usually consumed by another accelerating trains around, or stored by energy storage devices. Therefore, the application of energy storage devices, such as on-board energy storage devices (OESDs) and substation-based energy storage devices, are becoming popular in recent years [4], [5]. When more integrated systems within which each subsystem is more closely interconnected e.g. OESDs, train control and timetabling, the integrated study plays a more effective role in energy saving and emission reduction as all subsystems are taken into account.

Batteries, flywheels and supercapacitors have been applied as OESDs in the urban rail transit and battery driven light rail is already in service in Canada [4]. Hybrid system is also utilized and it is a combination of different OESDs, such as batteries and supercapacitors, to achieve suitable power rating and energy capacity [6]. Some studies have already indicated that OESD has evident effect on reducing energy consumption [7]–[9]. To theoretically analysis the performance of the utilized OESDs, the modeling and simulation on the configuration of OESDs are conducted by many researchers. By employing the Modelica language, high-power lithium batteries and supercapacitors as OESDs for trams are modeled and simulated in [10], where a cost/benefit analysis is achieved. By using the equivalent-electric-circuit-based approach, the lead-acid battery, supercapacitor and their hybrid model are all established and tested in automotive applications [11]. In both [12] and [13], the control strategies of the supercapacitor as OESD for electric trains are investigated, where the reference rule-based OESD control is achieved. A power and capacity-constrained configuration methodology (PC-Method) is proposed in [14] to configure the on-board supercapacitor array for recovering more regenerative braking energy. By considering the influence of different types of OESD on energy consumption, the mathematical-programming-based method is proposed to model

the supercapacitor, Li-ion battery and flywheel to obtain their optimal size [15] to minimize the energy consumption of the train operation. Also, the hybrid traction system with fuel cell and battery on rail vehicles is also investigated in [16], focusing on the feasibility of its application.

To take the full advantages of OESD, the integrated optimization on train operation with OESD becomes increasingly popular in recent years. In addition, Sequential Quadratic Programming (SQP) is used in [17] to optimize the train speed profile between two stations with OESD of fixed initial voltage and terminal voltage level, and the objective of it is to minimize the energy consumed from the substations considering state of charge (SOC) of OESD. As a popular method, DP approach is employed in [18] to optimize the speed profile of the train with supercapacitor for an entire real-world line from the initial station to the terminal station of both directions. Based on the Mixed Integer Linear Programming (MILP), the state of energy (SOE) of OESD is introduced and an integrated optimization model is proposed to optimize train speed profile under constraints of OESD capacity, initial state of energy (ISOE) and degradation from the viewpoint of energy flow scope [19]. The model is extended in [20] and the OESD is given the freedom to charge or discharge at the intermediate station. Based on the industrial information, the speed profile optimization problem for catenary-free train with lithium-ion batteries is considered in [21], where a battery-driven train designed by Bombardier Transportation and tested in UK is studied. The tram speed profile optimization with onboard supercapacitor is also explored in [22] with consideration of the road signaling systems based on DP, where the partially electrified track is studied. Considering the different dynamic power limits of supercapacitors, flywheels and Li-ion batteries, the integrated optimization on train speed profiles with three above types of OESDs has been investigated in [23], where the energy-saving potential comparisons among different types of energy storage as OESD are also given.

Some researchers found that only optimizing the train speed profile or control strategy e.g. in [24]–[30] is not sufficient thus the integrated approach considering both the control and timetabling becomes the new direction in recent years. An iterative method is proposed to optimize both the running time and train speed profile together to save total traction energy consumption of the whole metro line [31]. Regenerative energy is also considered in the integrated approach, in [32] the integrated optimization on the train operation timetable is investigated by maximizing the overlapped time for acceleration and braking events to make the most of the regenerative energy for reducing the net energy consumption. The analytical method is also used in figuring out this combined problem and this method is used to optimize the train speed profiles i.e. speed between switching points, and schedule i.e. the departure time and arrival time of each station are optimized for saving more net energy consumption [33]. High-speed railway corridor is also studied and a DP solution algorithm is proposed to find the speed/acceleration profile solutions with dualized train headway and power supply constraints [34]. A three-dimensional space-time-speed grid networks is established to characterize both

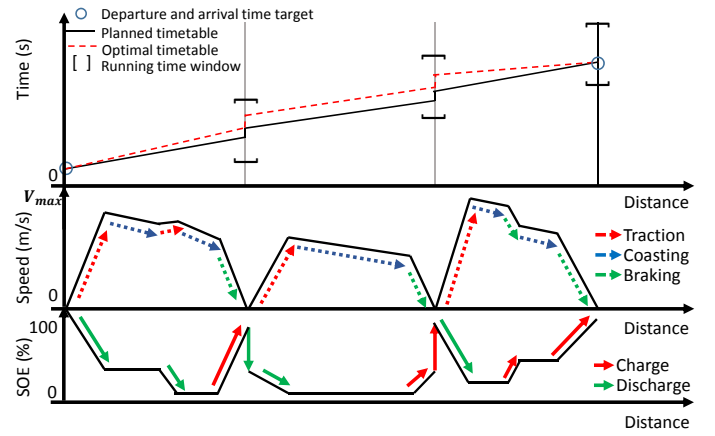


Fig. 1. Illustration of the expected optimized timetable, train operation and OESD management with a 4-station simple case by using the proposed method. The speed and SOE profiles at the bottom indicate that the OESD is closely interacting with the train speed profiles and timetable. OESD supports the traction and receives the regenerative energy for each inter-station journey and it takes an active charging and discharging control on the SOE when the train dwells at each station.

second-by-second train trajectory and segment-based timetables at different space and time resolutions. Recently, the optimal multi-train speed profiles optimization and timetable design is considered in [35] to reduce traction energy consumption based on real-world case study. Except the DC railway systems, the integrated train speed profiles and timetable optimization for AC railway systems are also explored in [36] to achieve the minimum electrical energy consumption.

It is found that some researchers have explored the area to make contribution to optimize the train operation considering OESD. Additionally, integrated optimization on the train speed profile and timetable is also becoming popular as discussed in the aforementioned contents. However, in the existing papers related to train operation with OESD, the timetable optimization problem is not explored and for the research with regard to the integrated optimization on train operation and timetable, the OESD is not involved. This indicates that the integrated optimization considering train operation, timetabling and management of OESD is still rare in the field. On the other hand, the energy status of OESD is found to affect energy consumption of train operation significantly [19], [37], showing the energy-saving potential of combination of these three components.

The work of this paper is an extension of [19] and [20] which only dealt with the optimal train operation with OESD limited in journeys with single or a few inter-station sections in a small scale. This paper discusses an integrated optimization on train operation, timetable and OESD discharging/charging strategy with a large scale. Compared to [19] and [20], the present paper has two improvements: (1) The ISOE of OESD before departure of the train at each station and the running time for each inter-station journey are no longer regarded as parameters but the decision variables. It expands the solution space to further minimize the net energy consumption, which is the difference of traction energy consumption and regenerative energy received by OESD. (2) The two-step algorithm proposed

can efficiently solve the optimization problem for train operation with OESD for multiple inter-station runs. The work in this paper has two main contributions to the field as follow:

- A concurrent optimization problem on OESD charge/discharge strategy, train speed profile and timetable has been solved in a large scale scenarios with multiple inter-station sections.
- A two-step algorithm is set up to significantly enhance the computational efficiency with Step 1 to store the optimization data fitted into convex functions which is solved in Step 2 using convex optimization.

Contribution 1 is related to the problem novelty. To the best of our knowledge, the work in this paper is the first of its kind in the area to optimize concurrently the running time, train speed profiles and energy status, i.e. ISOE in the research, of OESD together to further reduce the net energy consumption of the railway system. Contribution 2 is related to the novelty of the proposed method. With the proposed two-step algorithm, when dealing with the real-world case in large scale with different route conditions, operational constraints, rolling stocks and OESD characteristics, the proposed approach can deliver the solutions efficiently. In terms of implementation, the solution brought by the proposed method will not disrupt the current systems due to a number of introduced constraints ensuring the compulsory operational requirements. It provides optimal power management strategies on traction-energy-related systems by not influencing other systems in line on the trains.

To show clearly the research scope and outcome, Figure 1 presents the resulted solution of a simplified case with 4 stations. In the study, the departure and arrival target time from the initial station to the terminal station is fixed and follows the practical timetable to not influence the traffic capacity of the whole line. The optimal running time, train speed profile, OESD discharge/charge profile for each inter-station journey and optimal SOE adjustment for OESD at each station are obtained by employing the proposed approach. The train conducts traction, coasting or braking during the running and OESD can support the traction and receive regenerative energy during the journey. The paper assumes the time consumed by the OESD's discharge/charge process is less than the dwell time, which is regarded fixed and not the variable to be optimized. In addition, when OESD is charged or discharged at station, the transmission loss is ignored because the electrical energy can be charged into the OESD or consumed by auxiliary devices on train or at station with relatively high efficiency thus net energy consumption of the whole system at station could be regarded as zero when compared with the inter-station energy cost [20].

The remainder of the paper is organized as follows: Section II discusses the formulation of the approximating function to describe the relationship between minimum energy consumption, running time and ISOE, in which its properties of convexity and verification are shown. Based on the results from Section II, Section III is to show the optimization procedure of the proposed approach. In Section IV, the real-world case based on Beijing Yizhuang Metro Line is investigated. Section V draws the conclusions and discusses the future work.

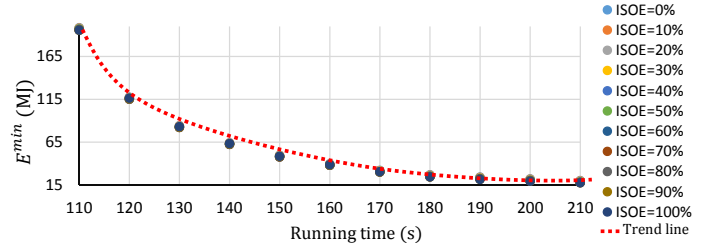


Fig. 2. The minimum net energy consumption based on different running time in a specific inter-station section. The trend line shows minimum net energy consumption are all monotonically decreasing under different given ISOE.

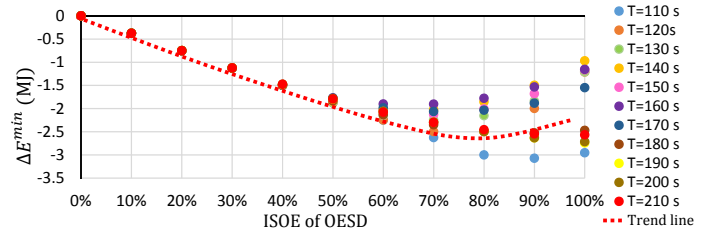


Fig. 3. The variation of minimum net energy consumption based on different ISOE in a specific inter-station section. The trend line shows that these variations drop first then rise for different given running time.

II. MINIMUM NET ENERGY CONSUMPTION APPROXIMATION AND MODELING

A. Approximating function formulation

Here a special case is used to show the key deduction of the proposed approach by applying the MILP model [19] in single inter-station scenario. In the case the track length is 3000 m, train mass is 178 t, OESD (supercapacitor) capacity and mass is 8.3 kWh (30 MJ) and 1.6 t, maximum traction/braking force and power is 200 kN and 5000 kW, maximum acceleration/deceleration is 1.2 m/s^2 and running time window is from 110 s to 210 s. The results are shown in Figure 2 and Figure 3.

When the running time increases, the minimum traction energy consumption of the train drops, which has been commonly recognized in the field of study [31] and [1]. In the research [19], it is also found that even with the OESD, the minimum net energy consumption will be reduced significantly when the running time in a specific inter-station section increases. The minimum net energy consumption is denoted as E_i^{min} and Figure 2 demonstrates the change of it resulted from different running time under specific ISOE of OESD. As a result, the relationship between E_i^{min} , which is the minimum net energy consumption for specific inter-station section i , and running time T can be firstly approximated to be in inverse proportion with some modifications as function f_i in (1), thus it has:

$$E_i^{min} \approx f_i(T) = P_{1,i} + \frac{P_{2,i}}{T + P_{3,i}} \quad (1)$$

where $P_{1,i}$, $P_{2,i}$ and $P_{3,i}$ are the constant for specific inter-station section i .

In a specific inter-station operation, the variation of minimum net energy consumption ΔE_i^{min} with respect to different given ISOE under certain running time is investigated. From Figure

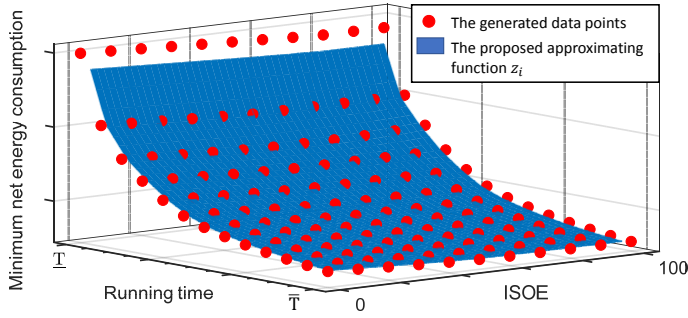


Fig. 4. An illustration of data points generated and the proposed approximating function $z_i(T, ISOE)$ in the form of (3)

3 it is found that when ISOE changes from 0% to 100%, the ΔE_i^{min} is always negative and decreases first then rises again. This result is also observed in the simulation of the operation of the train equipped with on-board batteries [37]. For all the running time in this specific inter-station operation, this trend remains similar though with slight discrepancies. As a result, the trend is modeled as a quadratic function, as the red dash line in Figure 3. Therefore, the relationship between the ΔE_i^{min} , which is the variation of minimum net energy consumption for a specific inter-station section i , and ISOE of OESD under different running time satisfies the following function g_i in (2):

$$\Delta E_i^{min} \approx g_i(ISOE) = P_{4,i} \times ISOE + P_{5,i} \times ISOE^2 \quad (2)$$

where $P_{5,i}$ is the constant parameters for linear term and quadratic term respectively for a standard quadratic function form in specific inter-station section i . The approximating function has no parameter of zero order because when $ISOE = 0$, ΔE_i^{min} is normally 0.

Figure 2 and Figure 3 are two projected planes from the direction of x-axis being the running time T and y-axis being the ISOE of OESD for specific inter-station operation, and the data group $(E_i^{min}, T, ISOE)$ in general situation with the running time window (\underline{T}, \bar{T}) is shown in Figure 4. To find the approximating function $z_i(T, ISOE)$ to fit the data group, (1) and (2) are summed up directly to do the reformulation of the function, as shown in (3).

$$z_i = P_{1,i} + \frac{P_{2,i}}{T + P_{3,i}} + P_{4,i} \times ISOE + P_{5,i} \times ISOE^2 \quad (3)$$

where $P_{1,i}, P_{2,i}, P_{3,i}, P_{4,i}$ and $P_{5,i}$ need to be calibrated in data fitting process using the results of specific inter-station section i .

The reason for forming (3) is that the E_i^{min} for one specific running time T while $ISOE=0$ is regarded as the basis, when the value of ISOE is changed, it is easy to observe that the corresponding negative ΔE_i^{min} can be simply added to E_i^{min} , showing that the sum of $f_i(T)$ and $g_i(ISOE)$ can approximate the minimum net energy consumption.

B. The verification of the proposed approximation

Since only a specific inter-station section and fixed OESD properties are used to show the deduction of the approximating

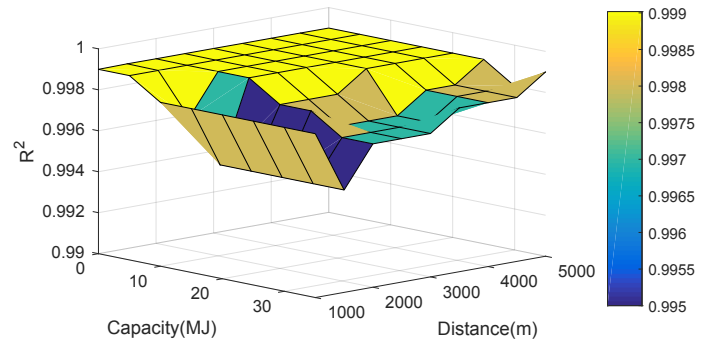


Fig. 5. The performance of the proposed approximating function when given different OESD capacity and different track length. The minimum value of R^2 is observed to be 0.995.

function (3), verification of the proposed approximation function is needed. For doing this, 9 different distances of inter-station journey from 1000 m to 5000 m with an increment step of 500 m and different OESD capacity from 1 MJ to 35 MJ with an increment step of 5 MJ as two components are selected. Different running time windows are also given to different track length.

By employing the MILP model [19] based on the above different inter-station information and energy storage information, the performance of the approximating function can be obtained followed by the data fitting process. Figure 5 shows the coefficient of determination R^2 of the verification with the minimum value of 0.995 and maximum value of 0.999. It means that though it is with some minor fluctuation of R^2 , using function (3) to approximate the relationship among minimum net energy consumption, running time and ISOE of OESD is reasonable, feasible and with a satisfactory modeling precision.

C. Convexity proof of the proposed approximating function

In the above sections, it has been demonstrated that using data fitting, the approximating function z_i can be built up. In this section, a proof of convexity of z_i will be conducted by using basic mathematical theory. The proof of convexity will directly lead to the global optimum of the results to be achieved by convex programming.

The Hessian matrix or Hessian is a square matrix of second-order partial derivatives of a scalar-valued function, or scalar field. It describes the local curvature of a function of many variables. The Hessian matrix is often used to determine the convexity of the given functions. A function $f(x)$ is strictly convex if or only if its Hessian matrix H is positive definite for all of the x in the domain [38]. The Hessian matrix of the approximating function $z = z(x, y) = P_1 + \frac{P_2}{x+P_3} + P_4 \times y + P_5 \times y^2$ is shown as below:

$$H_z = \begin{bmatrix} \frac{2P_2}{(x+P_3)^3} & 0 \\ 0 & 2P_5 \end{bmatrix}$$

The Hessian matrix is positive definite if and only if its n leading principal minors are greater than 0, which means that

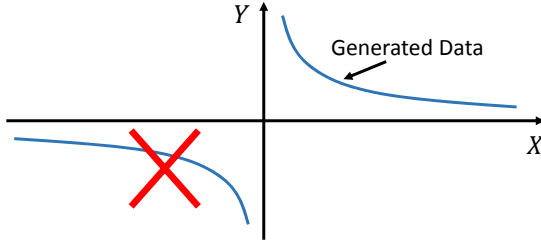


Fig. 6. The property of relationship between running time and minimum energy consumption extracted by the generated data. The generate data can only form the curve in first quadrant but not the curve in third quadrant.

the components in the matrix need to satisfy the three conditions shown in (4).

$$\begin{cases} \frac{2P_2}{(x+P_3)^3} > 0 \\ 2P_5 > 0 \\ \frac{2P_2}{(x+P_3)^3} \times 2P_5 - 0 > 0 \end{cases} \quad (4)$$

From the property of the inversely proportional function in relationship between E_i^{min} and T , it can be deduced that the parameter P_2 is positive. The reason for this is because the inversely proportional function is a strictly monotone decreasing function, the first-order derivative of it should greater then 0:

$$\begin{aligned} \therefore \frac{\partial z}{\partial x} &= -\frac{P_2}{(x+P_3)^2} < 0 \\ \therefore P_2 &> 0 \end{aligned}$$

In addition, another important property of the inversely proportional function is that it contains a pair of centrosymmetric curves, as the blue curves shown in Figure 6. If $Y = y - P_1$ and $X = x + P_3$, under the realistic train operation, the fitting curve representing the relationship between running time and minimum energy consumption can only form the right-sided curve located in the first quadrant but not the left-sided curve located in the third quadrant (Figure 6), thus it has:

$$\begin{aligned} \therefore X &> 0, Y > 0 \\ \therefore x + P_3 &> 0, y - P_1 > 0 \\ \therefore (x + P_3)^3 &> 0 \end{aligned}$$

On the other hand, it is easily known that P_5 is always greater than 0 because the ΔE_i^{min} sees a decrease trend first then rises again (Figure 3), which means that this parameter for the quadratic function is positive.

As a result, H_z is positive definite, which means the proposed approximating function z_i is strictly convex. In addition, one of a very important properties of convex function is that if z_1, z_2, \dots, z_n are all convex, the sum of them $\sum_{i=1}^n z_i$ is convex as well. Moreover, the convexity of the function also tells that this function has global minimum point.

III. A TWO-STEP APPROACH

The proposed approach consists of two steps, one is the preprocessing step (Step 1) and the other is the solving step

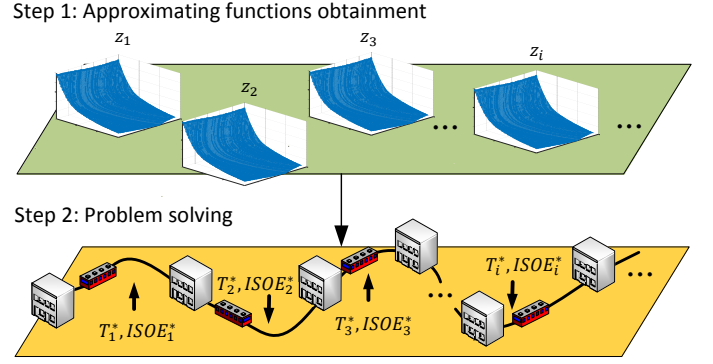


Fig. 7. The schematic of the proposed two-step method. In Step 1, the approximating functions z_i of all the studied inter-station operations are obtained. In Step 2, convex optimization problem is established and solved to obtain the optimal running time allocation and ISOE of each inter-station journey ($T_i^*, ISOE_i^*$)

(Step 2), as shown in Figure 7. Step 1 is the bottom level which generates, collects the data and builds the approximating functions to describe the relationships between the minimum net energy consumption, running time and ISOE of OESD. Since each inter-station section has its own route conditions e.g. speed limits or gradient information which usually stay fixed once the construction and rolling stock is finished and confirmed. By inputting different journey time T from the lower boundary \underline{T} to the upper boundary \overline{T} with a preset step length e.g. 5 s and different ISOE from 0 to 100% with a preset step length e.g. 10% in the MILP model [19] repeatedly, the minimum net energy consumption data group ($E_k^{min}, T_k, ISOE_k$) for specific inter-station section i can be generated and collected. After having the data group for each inter-station operation, the data fitting can be applied by using the proposed approximating function form shown in (3). The data fitting process is repeated until this work for all of the inter-station sections are finished then all of the approximating functions z_i are obtained.

After the procedure in Step 1, when the approximating functions z_i for all of the inter-station sections of the studied railway line are obtained, procedure of Step 2 is conducted. In Step 2, allocation of the running time for each inter-station operation and management of the ISOE of OESD of each inter-station operation with relevant constraints arising from the operation of OESD and the train can be conducted. The total operation time from the initial station to the terminal station needs to be determined to ensure sufficient service capacity in real operations, the constraint of which is added as (5)

$$\sum_{i=1}^n T_i = T_t \quad (5)$$

where n is the total number of the inter-station section of the whole journey, T_i is the running time for inter-station section i and T_t is the total running time for the whole journey. Additionally, the running time for each inter-station operation needs to be in a preset running time window, thus the constraint (6) is added as below.

$$\underline{T}_i \leq T_i \leq \overline{T}_i \quad (6)$$

where \underline{T}_i and \overline{T}_i are the lower and upper boundaries of the running time window for i^{th} inter-station run. Due to the capacity limit of the OESD, for each inter-station journey, the constraints (7) need to be satisfied.

$$0 \leq ISOE_i \leq 100\% \quad (7)$$

where $ISOE_i$ is the ISOE for inter-station operation i .

The target is to find out the optimal train speed profile, timetable and ISOE for each inter-station operation with minimized total net energy consumption of all the inter-station operations, Thus the optimization problem is formulated as shown in (8):

$$\begin{aligned} \min_{(T_i, ISOE_i)} \quad & \sum_{i=1}^n z_i \\ \text{s.t.} \quad & (5) - (7). \end{aligned} \quad (8)$$

Since both the objective function and constraints are all convex, a constrained convex optimization problem will be formulated based on the outcomes of Step 1.

After optimization in Step 2, a set of optimal $(T_i^*, ISOE_i^*)$ can be obtained and allocated. Then $(T_i^*, ISOE_i^*)$ can be substituted in the MILP model in [19] to obtain the detailed optimal train speed profile and optimal discharge/charge strategy for OESD of each inter-station section i .

IV. CASE STUDIES AND RESULTS DISCUSSION

In this section, the proposed approach is firstly conducted on the general case to show the effectiveness and flexibility of the method. After the general case study, the method is applied on a real-world metro line: Beijing Yizhaung Line to show the robustness of the proposed model as well as to provide a detailed illustration on how to allocate the running time and manage the OESD well for energy reduction in a real-world case. Noted that the case studies are conducted by using Matlab R2018b and CPLEX 12.8.0 solver on a PC with Intel Core i5-6500 processor (3.20 GHz) and 8.00 GB RAM.

A. General Case Studies

The general case studies are to present the effectiveness of the proposed method on dealing with the optimization problem under various conditions. The maximum traction/braking force and power of the train vehicle used in general case studies are set to be 200 kN and 5000 kW with the OESD capacity being 30 MJ. The track is set to be flat without slope and speed limits.

Firstly, scenarios with different ISOE of the OESD, which are 30%, 80% and 100%, for a general inter-station operation, are conducted and compared, as shown in Figure 8. The running time for this case is 105 s and the track length is 1800 m. The black solid line is the optimal train speed profile obtained by using the proposed approach. It is easily observed that train speed profiles and discharge/charge strategies of OESD are notably different due to the influence of the ISOE of OESD. The OESD should be charged to reach the optimal ISOE which is 57.0% before the train departs. When the train accelerates, the OESD is used to assist this motion, followed by slight

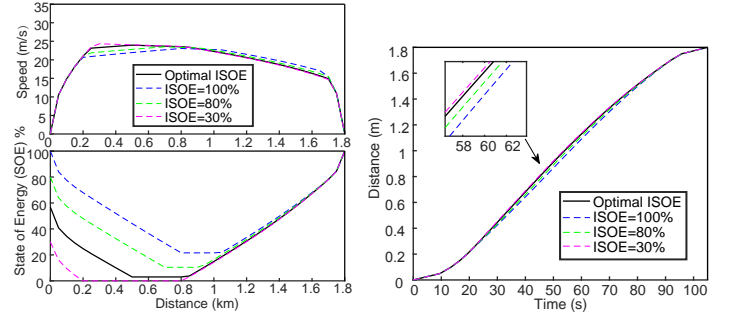


Fig. 8. The optimal train speed profiles, discharge/charge management and timetable for a general single inter-station operation.

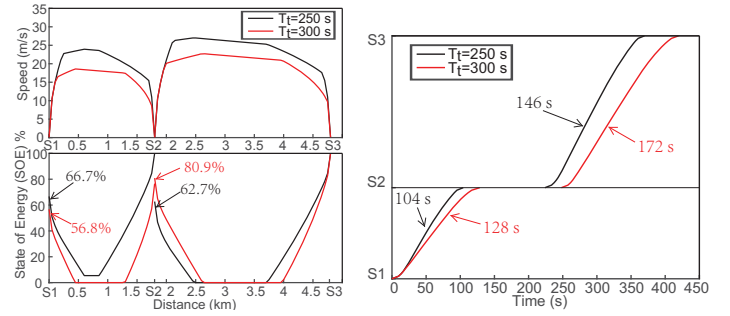


Fig. 9. The optimal train speed profiles, discharge/charge management and timetable for a general 3-station route with different total running time T_t (The sudden change of the SOE at the station represents the adjustment of SOE at each station).

acceleration motion until the OESD is fully utilized then the train starts to coast. The OESD is charged to be 100% when the train finishes the trip. As for the scenarios with respective ISOE, the train operations see different strategies, e.g. longest acceleration distance for case with ISOE=100% and longest braking distance for case with ISOE=30%. The discrepancies of the running time can also be observed when ISOE is different.

Normally different railway line has different operational requirement on timetable. In this case, here a general 3-station route with the total running time T_t set to be 250 s and 300 s respectively is investigated to understand how the model deal with different operational constraints. The results have been shown in Figure 9, and the optimal speed profiles and the optimal ISOE for both journeys of both scenarios are significantly different due to the change of T_t from the initial station to the terminal station. For instance, at the intermediate station, for scenario with $T_t = 250$ s the OESD needs to be discharged to decrease its SOE by 38.3% to reach the optimal ISOE for the next inter-station journey, which is 62.7%. For the scenario with $T_t = 300$ s the optimal solution is to charge the OESD and raises its SOE by 4.3% to reach the ISOE of 80.9%. The results indicate that different T_t brings different optimal strategies of both train operation and OESD management when the OESD is allowed to adjust its SOE during dwelling.

Different OESD specs will also lead to different optimal solutions, and the scenarios on the a general 3-station route

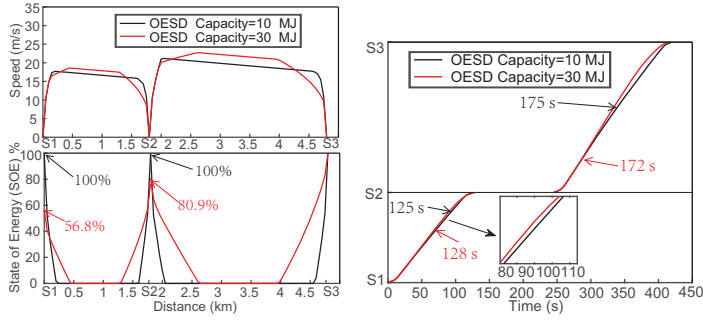


Fig. 10. The optimal train speed profiles, discharge/charge management and timetable for a general 3-station route with different OESD capacity (The sudden change of the SOE at the station represents the adjustment of SOE at each station).



Fig. 11. The route map of Beijing Yizhuang Line

with different capacities of OESD being 10 MJ and 30 MJ respectively are given to show this influence. The total running time T_t is fixed to be 300 s and the results are shown in Figure 10. It can be found that the optimal running time allocation, train operation and OESD operation are changed due to the influence of different OESD capacity. For the train equipped with OESD whose capacity is 10 MJ, the optimal ISOE of both inter-station operations are all 100% and at the end of the journey the OESD is fully charged by the regenerative energy. As a result, the OESD does not need to discharge or charge at station 2.

In summary, the general case studies above show that the mutual influences among train operation, timetabling and OESD discharge/charge management exist. Additionally, it can also be told that the proposed method can deal with the systems with different parameters and specs, which shows the effectiveness and robustness of the approach.

B. Real-world Case: Beijing Yizhuang Line

Yizhuang Line has 14 stations, 1 depot and the total length of line is more than 22 km, see Table I. For each inter-station section, the running time windows are different according to corresponding track length, system capacity and passenger demand, and the practical total running time for each direction, i.e. upline and downline, is 1620 s (27 minutes) respectively. The gradient change, speed limits, traction/braking force and train drag force are all shown in Figure 12. Train mass is 194.3 t, maximum acceleration/deceleration rate is 1.2 m/s^2 ,

TABLE I
THE OPERATIONAL INFORMATION OF YIZHUANG LINE

Start station	End station	Track length (m)	Running time windows (s)		Practical running time (s)	
			T_I	T_I	upline	downline
SJ	XC	2631	160	220	188	190
XC	XH	1274	82	138	106	103
XH	JG	2366	82	177	156	153
JG	YZQ	1983	117	152	133	133
YZQ	WH	992	68	120	84	84
WH	WY	1539	97	123	112	112
WY	RJ	1280	80	133	95	98
RJ	RC	1354	83	134	101	102
RC	TJ	2337	150	185	161	158
TJ	JH	2265	138	171	147	147
JH	CQN	2086	142	179	137	139
CQN	CQ	1287	80	132	98	98
CQ	YZ	1334	84	135	102	103
SUM		22728			1620	1620

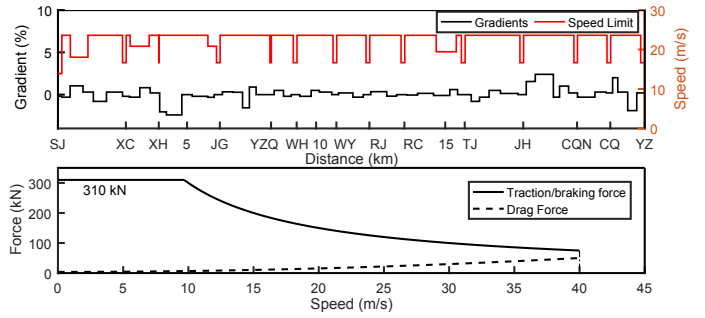


Fig. 12. The route and traction/braking conditions of Yizhuang Line

OESD capacity is 11.1 kWh with a mass of 2.2 t and the maximum charge/discharge power being 500 kW. With the provided information above, the preprocessing in Step 1 will be conducted for all inter-station sections. It should be noticed that due to the different direction of movement of the train, the optimal train operation of each inter-station section on upline and downline will change due to different speed limits and gradients. This requires the preprocessing work to extend to 26 inter-station operations for both directions. Table II tabulates the results of the preprocessing work at Step 1 and the performances of the approximation for each inter-station operation of both direction are considered satisfactory with the minimum R^2 being 0.998 for inter-station operation YZQ-WH and WH-YZQ, which also shows the robustness of the proposed approximation in dealing with the real-world problem.

The optimal running time allocation for the whole line and the optimal ISOE of OESD for each inter-station operation are listed in Table III. It is easily observed that the optimal running time allocation yielded by the proposed approach has significant discrepancies when compared to the practical running time and the offsets are also given in the parenthesis. Based on that, the comparison between the optimal timetable and practical one are presented in Figure 13. In addition, though the total running time for upline and downline is the same, the running time allocation is different. Similarly, the optimal ISOE for the same inter-station section is also different for upline and downline operation. After obtaining optimal solution of running

TABLE II

THE RESULTS OF STEP 1 FOR UPLINE AND DOWNLINE OF YIZHUANG LINE

Inter-station operation	P_1	P_2	P_3	P_4	P_5 ($\times 10^{-4}$)	R^2
SJ-XC	15.90	1470.42	-129.76	-0.06	2.15	0.999
XC-XH	4.33	613.92	-68.81	-0.05	3.85	0.999
XH-JG	4.97	2327.42	-94.88	-0.06	3.36	0.999
JG-YZQ	4.00	1747.21	-84.35	-0.06	4.01	0.999
YZQ-WH	0.37	548.51	-55.51	-0.04	3.48	0.998
WH-WY	-0.31	1283.22	-70.31	-0.06	4.12	0.999
WY-RJ	1.40	807.40	-64.97	-0.05	3.91	0.999
RJ-RC	1.88	869.05	-67.62	-0.05	3.97	0.999
RC-TJ	0.54	3208.89	-81.39	-0.06	3.31	0.999
TJ-JH	3.23	2552.20	-87.06	-0.06	3.44	0.999
JH-CQN	8.33	1710.89	-90.62	-0.06	3.64	0.999
CQN-CQ	1.22	826.23	-64.91	-0.05	3.92	0.999
CQ-YZ	1.32	879.97	-66.58	-0.05	3.95	0.999
YZ-CQ	0.95	891.92	-66.45	-0.05	3.92	0.999
CQ-CQN	1.27	824.89	-65.01	-0.05	3.91	0.999
CQN-JH	8.65	1658.26	-90.77	-0.06	3.69	0.999
JH-TJ	3.69	2174.83	-91.88	-0.06	3.48	0.999
TJ-RC	7.08	2139.44	-97.89	-0.06	3.17	0.999
RC-RJ	2.03	854.84	-67.89	-0.05	3.94	0.999
RJ-WY	1.41	804.72	-65.06	-0.05	3.88	0.999
WY-WH	-0.33	1286.04	-70.34	-0.06	4.13	0.999
WH-YZQ	0.21	558.43	-55.22	-0.04	3.43	0.998
YZQ-JG	3.72	1770.66	-84.09	-0.06	4.00	0.999
JG-XH	6.16	2181.99	-97.49	-0.06	3.31	0.999
XH-XC	4.18	612.30	-68.80	-0.05	3.83	0.999
XC-SJ	12.15	2064.00	-115.74	-0.06	2.72	0.999

TABLE III

THE OPTIMISATION RESULTS FOR UPLINE AND DOWNLINE OF YIZHUANG LINE

Inter-station section	T^* (s)	$ISOE^*$ (%)	E^* (MJ)
SJ-XC	176 (-12)	79.5	43.55 (+6.48 ¹ , +2.29 ² , -4.25 ³)
XC-XH	99 (-7)	71.4	23.64 (+4.91 ¹ , +4.60 ² , -3.12 ³)
XH-JG	151 (-5)	81.3	43.03 (+3.22 ¹ , +2.00 ² , -7.45 ³)
JG-YZQ	140 (+7)	79.8	33.02 (-4.18 ¹ , -4.44 ² , -14.48 ³)
YZQ-WH	85 (+1)	65.4	16.29 (-1.32 ¹ , -1.10 ² , -14.48 ³)
WH-WY	120 (+8)	75.0	23.36 (-5.27 ¹ , -5.18 ² , -14.24 ³)
WY-RJ	99 (+4)	70.5	23.43 (-4.00 ¹ , -3.57 ² , -11.82 ³)
RJ-RC	104 (+3)	71.7	23.96 (-2.76 ¹ , -2.48 ² , -10.94 ³)
RC-TJ	160 (-1)	81.5	38.06 (+0.48 ¹ , +0.48 ² , -9.71 ³)
TJ-JH	143 (-4)	81.4	45.81 (+3.43 ¹ , +3.22 ² , -6.96 ³)
JH-CQN	143 (+6)	81.4	38.28 (-3.55 ¹ , -3.90 ² , -13.71 ³)
CQN-CQ	100 (+2)	70.6	23.26 (-1.62 ¹ , -1.38 ² , -9.57 ³)
CQ-YZ	101 (-1)	72.0	25.16 (+0.58 ¹ , +0.76 ² , -7.54 ³)
SUM	1620 (0)		400.85 (-3.60 ¹ , -8.70 ² , -122.68 ³)
YZ-CQ	104 (+1)	77.9	22.35 (-0.87 ¹ , -2.57 ² , -9.27 ³)
CQ-CQN	100 (+2)	76.3	22.63 (-2.23 ¹ , -2.00 ² , -10.31 ³)
CQN-JH	143 (+4)	88.7	37.81 (-2.12 ¹ , -2.22 ² , -12.32 ³)
JH-TJ	150 (+3)	88.7	40.29 (-1.82 ¹ , -2.48 ² , -12.71 ³)
TJ-RC	155 (-3)	89.2	40.76 (+1.51 ¹ , +1.00 ² , -8.92 ³)
RC-RJ	104 (+2)	77.4	24.11 (-1.56 ¹ , -1.38 ² , -9.89 ³)
RJ-WY	100 (+2)	76.1	22.37 (-2.04 ¹ , -1.83 ² , -10.07 ³)
WY-WH	115 (+3)	81.4	26.26 (-2.35 ¹ , -2.32 ² , -11.41 ³)
WH-YZQ	84 (0)	70.4	16.95 (-0.61 ¹ , -0.38 ² , -8.06 ³)
YZQ-JG	137 (+4)	86.7	34.88 (-2.27 ¹ , -2.28 ² , -12.58 ³)
JG-XH	155 (+2)	89.0	40.82 (-1.15 ¹ , -1.18 ² , -12.41 ³)
XH-XC	100 (-3)	76.3	22.32 (+2.29 ¹ , +2.29 ² , -6.24 ³)
XC-SJ	172 (-18)	88.5	44.70 (+8.47 ¹ , +7.03 ² , -1.63 ³)
SUM	1620 (0)		396.25 (-4.75 ¹ , -8.32 ² , -125.82 ³)

¹ The difference between optimal strategy and fully charged strategy² The difference between optimal strategy and no management strategy³ The difference between optimal strategy and situation without OESD

time and ISOE for each inter-station operation, they can be used as input of MILP model to yield the optimal train speed

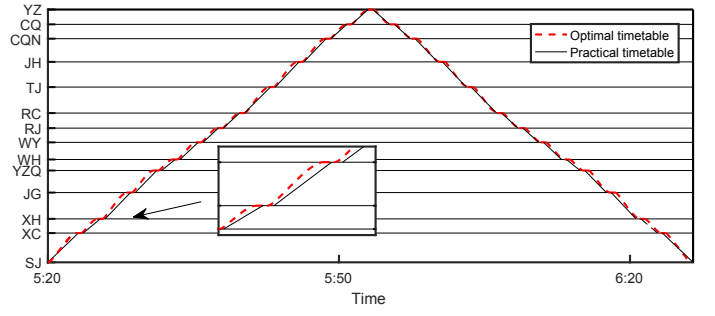


Fig. 13. The comparison between the resulted optimal timetable and practical timetable of Beijing Yizhuang line for one service cycle from 5:20 am.

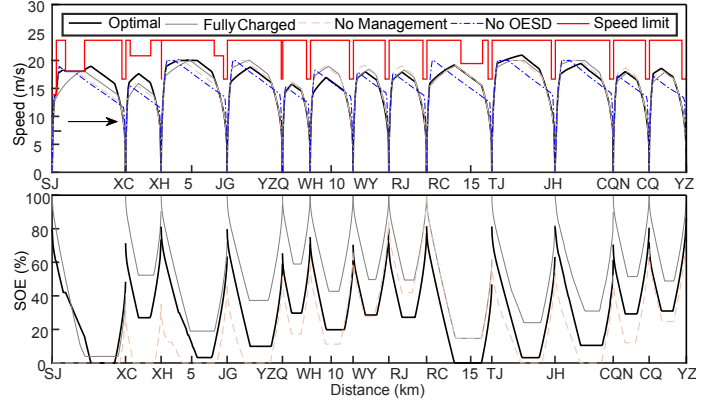


Fig. 14. The optimal speed profiles and discharge/charge management for upline operation (gap of the SOE represents the adjustment of SOE at each station)

profiles, optimal discharge/charge curves of OESD as well as the minimum net energy consumption from the initial station to the terminal station of the whole metro line. The total CPU time for obtaining the optimal solution is the sum of the time consumed on finding optimal (T_i^* , $ISOE_i^*$) for each direction and the time consumed on finding the optimal speed profile for each inter-station operation based on the resulted (T_i^* , $ISOE_i^*$). The CPU time is $0.08+38.78=38.86$ s for upline and $0.10+48.28=48.38$ s for downline, which shows the high computational efficiency of the proposed approach. This is resulted from the proposed approach where solving step can significantly enhance computational efficiency with much fewer decision variables and much less complex modeling using the data from the preprocessing step. For instance, for each running direction the optimization problem of this real-world case only consists of 26 variables (13 T_i and 13 $ISOE_i$) to be optimized in the objective function, 1 equality constraint ensuring the fixed total running time 1620 s and the lower/upper bounds of the variables guaranteeing their effective range, leading to a fast computing speed.

Figure 14 shows the optimal train speed profiles and optimal discharge/charge strategy of OESD for upline and the Figure 15 shows the both optimal curves for downline, referring to the black solid line in the figure. The net energy consumption of each station and both directions are tabulated in Table III. For each arrival station, OESD needs to adjust its SOE which has

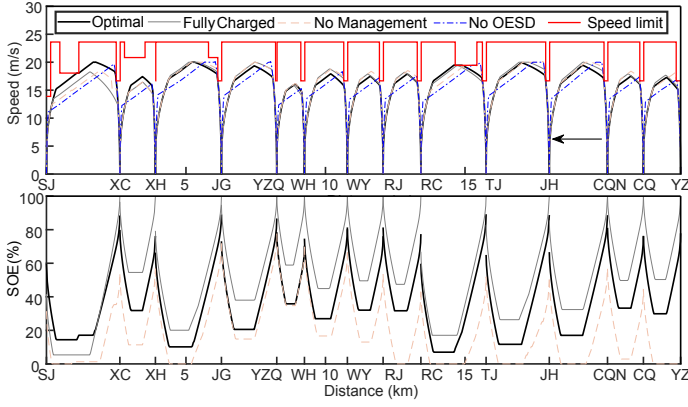


Fig. 15. The optimal speed profiles and discharge/charge management for downline operation (gap of the SOE represents the adjustment of SOE at each station)

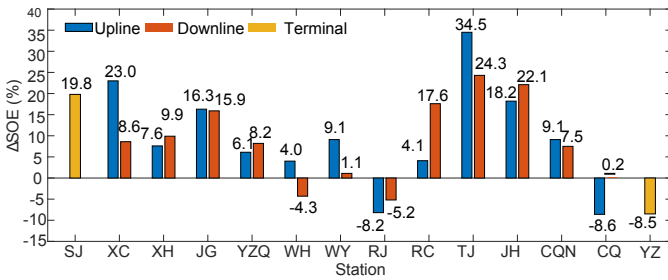


Fig. 16. The optimal SOE adjustment value for OESD at each station, where the positive values mean that the OESD needs to charge the corresponding SOE when dwelling and negative values mean that the OESD needs to discharge the corresponding SOE.

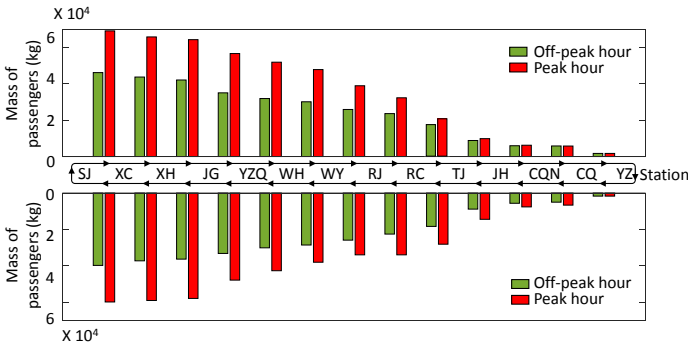


Fig. 17. The average mass of the passengers for all of the inter-station sections during "off-peak hour" and "peak hour".

been shown as the gap of the SOE at each station in Figure 14 and Figure 15. The value for the gap is the difference between the terminal SOE of the last inter-station journey and the optimal ISOE of the next inter-station journey.

For showing the effectiveness of the proposed approach, three scenarios: "Fully Charged", "No Management" and "No OESD", are selected to make comparison with the proposed optimal strategy based on this real-world metro line, referring to the gray, brown and blue lines in Figure 14 and Figure 15 as well. "No OESD" is to denote the scenario that there is no OESD installed on the train; "Fully Charged" is to represent that

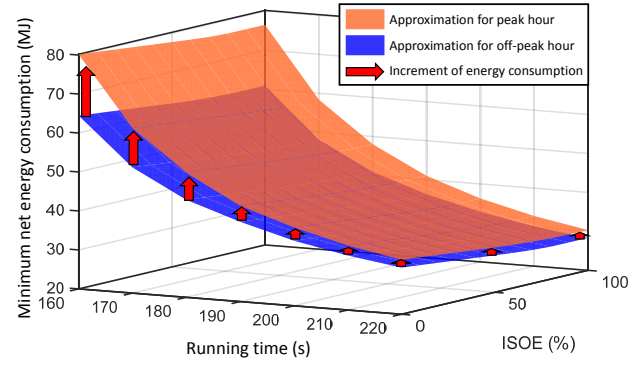
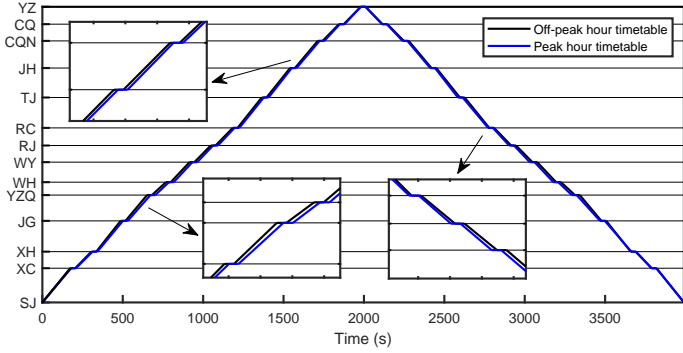


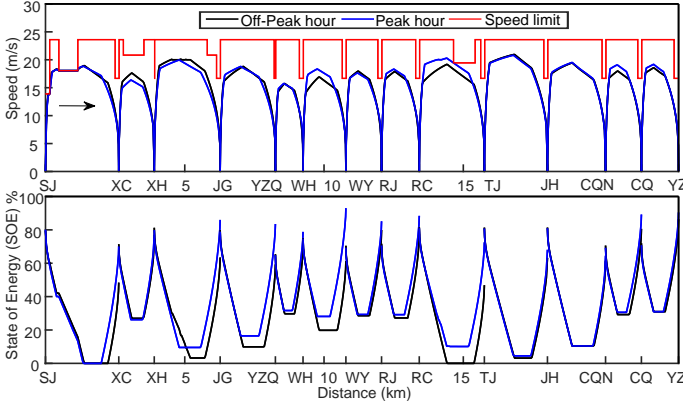
Fig. 18. An SJ-SC example for showing the change of the approximation of minimum net energy consumption when considering the different passenger demand.

the OESD is fully charged before the train departs from each station: "No Management" is to denote that OESD is empty at the first station and no discharge/charge behavior are allowed when train dwells at station, thus the terminal SOE of the OESD is the ISOE of the next inter-station operation. Both scenarios involving OESD have been studied in previous research [39] and [18] and show good energy-saving performance. "Fully charged", "No Management" and "No OESD" scenarios are all conducted following the practical running time. It is worth mentioning that for the "No OESD" scenario, the regenerative energy is not completely wasted but assumed to be utilized by the accelerating trains around, and the average recovering efficiency is set to be 30% according to the existing literature [1].

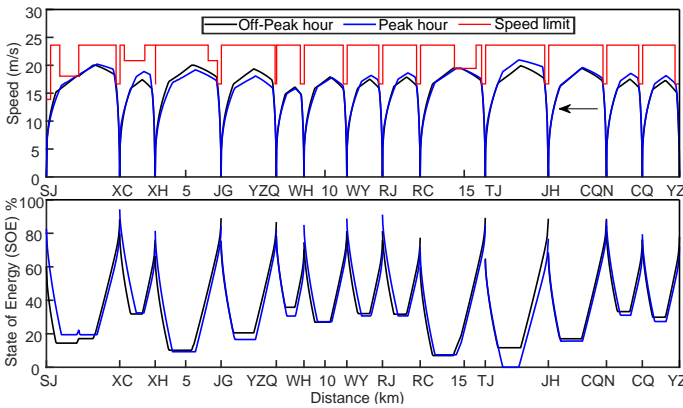
The speed profiles and discharge/charge behavior of these three scenarios and the optimal solution are significantly different. One thing should be noticed is that the optimal running time for WH-YZQ of the downline remains the same with the practical running time while the net energy consumption of the proposed optimal strategy is still lower than that of "Fully Charged" and "No Management" scenario, which shows the effectiveness of the proposed approach on OESD management to help reduce the energy consumption. Though for some inter-station operation, the proposed optimal strategy raises the net energy consumption, the total net energy consumption of each direction is minimized further, as shown in Table III. For the upline the net energy consumption is reduced by 3.60 MJ, 8.70 MJ and 122.68 MJ, which is 0.89%, 2.12% and 23.43%, and for the downline it is reduced by 4.75 MJ, 8.32 MJ and 125.82 MJ, which is 1.18%, 2.06% and 24.10% , compared to the "Fully charged", "No Management" and "No OESD" situations respectively. Therefore, for a service cycle of a single train, the net energy consumption can be saved by 1.04%, 2.09% and 23.77%. It can be seen that the energy consumption of the "No OESD" scenario is the highest among the optimal solution and other two scenarios, which implies that the installation of OESD has the most significant impact on the energy-saving effect. Also, by managing the ISOE and OESD power properly, the energy consumption can be reduced further by a relatively small but still effective value.



(a)



(b)



(c)

Fig. 19. The optimal solutions for both "off-peak hour" and "peak hour" operations and the corresponding comparison, (a): timetable, (b) and (c): train speed profiles and OESD discharge/charge management for upline and downline.

Figure 16 shows the adjustment value for the OESD at each station and it should be noticed that for upline and downline though at the same station it sees different management strategy i.e. charge by 4.0% SOE for upline operation and discharge by 4.3% for downline operation at RC, and different adjustment value i.e. charge by 34.5% SOE for upline operation and charge by 24.3% SOE for downline operation at TJ. Additionally, it can be noticed that when each train begins the first service cycle from SJ the OESD needs to be charged to 79.5% of capacity

assuming that the OESD is empty before the journey starts. Nevertheless, for the later service cycles, the OESD just needs to keep SOE to be 19.8% because the OESD has been charged by regenerative energy from the downline operation. Therefore, there are two special stations, SJ and YZ at both ends of the line, at which the OESD only has unique strategy regardless of the operating directions.

C. Considering Dynamic Passenger Demand

It can be observed that in real-world operations the passenger demand of the metro system is time-variant, which will lead to the different optimal solution for different time in one day. In the above case, only the optimal solution for off-peak time of Yizhuang Line from 5:20 am is investigated, for showing the flexibility and robustness of the proposed method, in this section the case with consideration of dynamic passenger demand will be conducted.

It has been found that though the passenger demand of the metro system is time-variant in one day, its daily pattern is similar for each day, thus the real-world metro operation of one day will be divided into "peak-hour" and "off-peak hour" operations. As shown in Figure 17, the average mass of passenger for Yizhuang Line with respect to all of the inter-station sections are investigated [40], the data of which will be used in Step 1 of our proposed method to generate the approximations of energy consumption. As an example, Figure 18 illustrates the change of the approximation in different period for SJ-*XC* inter-station operation. It can be found that consideration of the passenger demand will not influence the proposed modeling and solving procedure, and the only difference for the approximation of "peak hour" and "off-peak hour" lies on increment of the minimum net energy consumption resulted from the varied total mass of the train with in-vehicle passengers.

The optimal solution of the train timetable of the upline and downline, speed profiles for each inter-station operation and OESD discharge/charge strategy during each inter-station journey/at each station are obtained for both "peak hour" and "off-peak hour" operations. As Figure 19 shows, due to the difference of the passenger demand, the optimal solutions see difference in both period. The comparison between optimal timetable of each inter-station for "off-peak hour" and "peak hour" are presented in Figure 19(a), which shows that the proposed method reallocates the running time considering the impact of the passenger demand. Correspondingly, the optimal train speed profiles for both directions and OESD discharge/charge strategy change as well when comparing both operation period, as illustrated in Figure 19(b) and 19(c).

The case shows the robustness of the proposed method when dealing with the dynamic passenger demand of the railway system, and the modeling and solving process of two steps guarantees the efficient and effective obtainment of the optimal solutions

V. CONCLUSION AND FUTURE WORK

The paper proposes a two-step approach to concurrently optimize the train operation, timetable and energy management

strategy of the on-board energy storage device (OESD) to minimize the net energy consumption of the whole system. This novel two-step method is able to effectively address the up-rising challenging but also important issues when OESDs are deployed in the railway system operations. The resulted optimal train operation, timetable and energy management strategy of OESD reduces the net energy consumption by 1.04%, 2.09% and 23.77% of a service cycle for a single train when compared to "Fully Charged", "No Management" and "No OESD" scenario respectively. The proposed approach is also computationally efficient since the CPU time for obtaining the optimal solution for multiple inter-station sections of the entire metro line is less than 1 min, namely 38.86 s for the upline and 48.38 s for the downline.

In the future, the constraints of dwell time could be considered into the model to explore the influence of it on the optimal strategy. In addition, different dynamic characteristics e.g. the noise of the system condition during operation, service life degradation, power density and energy density of different types of OESD can also be taken into account to deal with various systems. The other one is to extend the approach to study the energy interaction among trains when OESD is involved, which might enhance the energy-saving effect with further system integration. Also, more detailed study might be achieved by integrating the information of smart grid, EV fleet or other systems. The investigation on the energy hub based on the railway station and regenerative energy is interesting and it is of great potential in the future.

REFERENCES

- [1] X. Yang, X. Li, B. Ning, and T. Tang, "A survey on energy-efficient train operation for urban rail transit," *IEEE Transactions on Intelligent Transportation Systems*, vol. 17, no. 1, pp. 2–13, 2016.
- [2] G. M. Scheepmaker, R. M. Goverde, and L. G. Kroon, "Review of energy-efficient train control and timetabling," *European Journal of Operational Research*, vol. 257, no. 2, pp. 355–376, 2017.
- [3] Z. Tan, S. Lu, K. Bao, S. Zhang, C. Wu, J. Yang, and F. Xue, "Adaptive partial train speed trajectory optimization," *Energies*, vol. 11, no. 12, p. 3302, 2018.
- [4] N. Ghaviha, J. Campillo, M. Bohlin, and E. Dahlquist, "Review of application of energy storage devices in railway transportation," *Energy Procedia*, vol. 105, pp. 4561 – 4568, 2017, 8th International Conference on Applied Energy, ICAE2016, 8-11 October 2016, Beijing, China.
- [5] G. Graber, V. Calderaro, V. Galdi, A. Piccolo, R. Lamedica, and A. Ruvio, "Techno-economic sizing of auxiliary-battery-based substations in DC railway systems," *IEEE Transactions on Transportation Electrification*, vol. 4, no. 2, pp. 616–625, 2018.
- [6] S. de la Torre, A. J. Sánchez-Racero, J. A. Aguado, M. Reyes, and O. Martínez, "Optimal sizing of energy storage for regenerative braking in electric railway systems," *IEEE Transactions on Power Systems*, vol. 30, no. 3, pp. 1492–1500, May 2015.
- [7] M. Dominguez, A. Fernandez-Cardador, A. P. Cucala, and R. R. Pecharroman, "Energy savings in metropolitan railway substations through regenerative energy recovery and optimal design of ato speed profiles," *IEEE Transactions on Automation Science and Engineering*, vol. 9, no. 3, pp. 496–504, July 2012.
- [8] A. M. Gee and R. W. Dunn, "Analysis of trackside flywheel energy storage in light rail systems," *IEEE Transactions on Vehicular Technology*, vol. 64, no. 9, pp. 3858–3869, 2015.
- [9] R. Takagi and T. Amano, "Optimisation of reference state-of-charge curves for the feed-forward charge/discharge control of energy storage systems on-board dc electric railway vehicles," *IET Electrical Systems in Transportation*, vol. 5, no. 1, pp. 33–42, 2015.
- [10] M. Ceraolo and G. Lutzemberger, "Stationary and on-board storage systems to enhance energy and cost efficiency of tramways," *Journal of Power Sources*, vol. 264, pp. 128 – 139, 2014.
- [11] S. Fiorenti, J. Guanetti, Y. Guezennec, and S. Onori, "Modeling and experimental validation of a hybridized energy storage system for automotive applications," *Journal of Power Sources*, vol. 241, pp. 112 – 120, 2013.
- [12] R. Takagi and T. Amano, "Optimisation of reference state-of-charge curves for the feed-forward charge/discharge control of energy storage systems on-board dc electric railway vehicles," *IET Electrical Systems in Transportation*, vol. 5, no. 1, pp. 33–42, 2015.
- [13] P. Arbolea, B. Mohamed, and I. El-Sayed, "Off-board and on-board energy storage versus reversible substations in dc railway traction systems," *IET Electrical Systems in Transportation*, vol. 10, no. 2, pp. 185–195, 2020.
- [14] X. Shen, S. Chen, G. Li, Y. Zhang, X. Jiang, and T. T. Lie, "Configure methodology of onboard supercapacitor array for recycling regenerative braking energy of urt vehicles," *IEEE Transactions on Industry Applications*, vol. 49, no. 4, pp. 1678–1686, 2013.
- [15] C. Wu, S. Lu, F. Xue, L. Jiang, and M. Chen, "Optimal sizing of on-board energy storage devices for electrified railway systems," *IEEE Transactions on Transportation Electrification*, pp. 1–1, 2020.
- [16] A. S. Abdelrahman, Y. Attia, K. Woronowicz, and M. Z. Youssef, "Hybrid fuel cell/battery rail car: A feasibility study," *IEEE Transactions on Transportation Electrification*, vol. 2, no. 4, pp. 493–503, 2016.
- [17] M. Miyatake and K. Matsuda, "Energy saving speed and charge/discharge control of a railway vehicle with on-board energy storage by means of an optimization model," *IEEJ Transactions on Electrical and Electronic Engineering*, vol. 4, no. 6, pp. 771–778, 2009.
- [18] Y. Huang, L. Yang, T. Tang, Z. Gao, F. Cao, and K. Li, "Train speed profile optimization with on-board energy storage devices: A dynamic programming based approach," *Computers and Industrial Engineering*, vol. 126, no. January, pp. 149–164, 2018.
- [19] C. Wu, W. Zhang, S. Lu, Z. Tan, F. Xue, and J. Yang, "Train speed trajectory optimization with on-board energy storage device," *IEEE Transactions on Intelligent Transportation Systems*, vol. 20, no. 11, pp. 4092–4102, 2019.
- [20] C. Wu, S. Lu, F. Xue, L. Jiang, and J. Yang, "Optimization of speed profile and energy interaction at stations for a train vehicle with on-board energy storage device," in *2018 IEEE Intelligent Vehicles Symposium (IV)*, June 2018, pp. 1–6.
- [21] N. Ghaviha, M. Bohlin, C. Holmberg, and E. Dahlquist, "Speed profile optimization of catenary-free electric trains with lithium-ion batteries," *Journal of Modern Transportation*, Jan 2019.
- [22] Z. Xiao, X. Feng, Q. Wang, and P. Sun, "Eco-driving control for hybrid electric trams on a signalised route," *IET Intelligent Transport Systems*, vol. 14, no. 1, pp. 36–44, 2020.
- [23] C. Wu, B. Xu, S. Lu, F. Xue, L. Jiang, and M. Chen, "Adaptive eco-driving strategy and feasibility analysis for electric trains with on-board energy storage devices," *IEEE Transactions on Transportation Electrification*, 2021.
- [24] A. Albrecht, P. Howlett, P. Pudney, X. Vu, and P. Zhou, "The key principles of optimal train control - part 2: Existence of an optimal strategy, the local energy minimization principle, uniqueness, computational techniques," *Transportation Research Part B: Methodological*, vol. 94, pp. 509 – 538, 2016.
- [25] —, "The key principles of optimal train control - part 1: Formulation of the model, strategies of optimal type, evolutionary lines, location of optimal switching points," *Transportation Research Part B: Methodological*, vol. 94, pp. 482 – 508, 2016.
- [26] S. Lu, S. Hillmansen, T. K. Ho, and C. Roberts, "Single-Train Trajectory Optimization," *IEEE Transactions on Intelligent Transportation Systems*, vol. 14, no. 2, pp. 743–750, jun 2013.
- [27] Y. Wang, B. De Schutter, T. J. J. van den Boom, and B. Ning, "Optimal trajectory planning for trains – A pseudospectral method and a mixed integer linear programming approach," *Transportation Research Part C: Emerging Technologies*, vol. 29, pp. 97–114, 2013.
- [28] P. Wang and R. M. Goverde, "Multiple-phase train trajectory optimization with signalling and operational constraints," *Transportation Research Part C: Emerging Technologies*, vol. 69, pp. 255–275, 2016.
- [29] X. Zhao, B. Ke, and K. Lian, "Optimization of train speed curve for energy saving using efficient and accurate electric traction models on the mass rapid transit system," *IEEE Transactions on Transportation Electrification*, vol. 4, no. 4, pp. 922–935, 2018.
- [30] Z. Tan, S. Lu, K. Bao, S. Zhang, C. Wu, J. Yang, and F. Xue, "Adaptive partial train speed trajectory optimization," *Energies*, vol. 11, no. 12, p. 3302, Nov 2018. [Online]. Available: <http://dx.doi.org/10.3390/en11123302>

- [31] S. Su, X. Li, T. Tang, and Z. Gao, "A subway train timetable optimization approach based on energy-efficient operation strategy," *IEEE Transactions on Intelligent Transportation Systems*, vol. 14, no. 2, pp. 883–893, 2013.
- [32] X. Li and H. K. Lo, "An energy-efficient scheduling and speed control approach for metro rail operations," *Transportation Research Part B: Methodological*, vol. 64, pp. 73 – 89, 2014.
- [33] —, "Energy minimization in dynamic train scheduling and control for metro rail operations," *Transportation Research Part B: Methodological*, vol. 70, pp. 269 – 284, 2014.
- [34] L. Zhou, L. C. Tong, J. Chen, J. Tang, and X. Zhou, "Joint optimization of high-speed train timetables and speed profiles: A unified modeling approach using space-time-speed grid networks," *Transportation Research Part B: Methodological*, vol. 97, pp. 157–181, mar 2017.
- [35] P. Wang and R. M. Goverde, "Multi-train trajectory optimization for energy-efficient timetabling," *European Journal of Operational Research*, vol. 272, no. 2, pp. 621–635, 2018.
- [36] Z. Pan, M. Chen, S. Lu, Z. Tian, and Y. Liu, "Integrated timetable optimization for minimum total energy consumption of an ac railway system," *IEEE Transactions on Vehicular Technology*, vol. 69, no. 4, pp. 3641–3653, 2020.
- [37] T. Sato and M. Miyatake, "A method of generating energy-efficient train timetable including charging strategy for catenary-free railways with battery trains," in *RailNorrköping 2019. 8th International Conference on Railway Operations Modelling and Analysis (ICROMA), Norrköping, Sweden, June 17th – 20th, 2019*, no. 69, 2019, pp. 995–1010.
- [38] S. Boyd and L. Vandenberghe, *Convex optimization*. Cambridge university press, 2004.
- [39] M. Miyatake, H. Haga, and S. Suzuki, "Optimal speed control of a train with on-board energy storage for minimum energy consumption in catenary free operation," *13th European Conference on Power Electronics and Applications 2009 EPE 09*, pp. 1–9, 2009.
- [40] X. Yang, A. Chen, B. Ning, and T. Tang, "A stochastic model for the integrated optimization on metro timetable and speed profile with uncertain train mass," *Transportation Research Part B: Methodological*, vol. 91, pp. 424–445, 2016.



train operation optimization, energy-saving strategies in transportation and smart transportation.

Chaoxian Wu was born in 1992 in Beihai, Guangxi, China. He received the BEng in Traffic Engineering from Tongji University, Shanghai, China, in 2015. He was awarded his Intercollegiate MSc degree in Transport & Sustainable Development from Imperial College London, UK and University College London, UK, in 2016. He is now pursuing the PhD of Electrical Engineering and Electronics from University of Liverpool, UK and also a Visiting Student with the South China University of Technology, Guangzhou, China.

His main research interests are railway engineering,



Electrical and Electronic Engineering. His main research interests include power management strategies, railway traction system, electric vehicles, optimization techniques and energy-efficient transportation systems.

Shaofeng Lu is currently an associate professor with the Shien-Ming Wu School of Intelligent Engineering (WUSIE), South China University of Technology (SCUT), China. Before joining SCUT in 2019, he spent 6 years as a faculty member with Department of Electrical and Electronic Engineering, Xi'an Jiaotong-Liverpool University (XJTLU), China. He received the BEng and PhD degree from the University of Birmingham in 2007 and 2011 respectively. He also has a BEng degree from Huazhong University of Science and Technology, Wuhan, China. All are in



with the Department of Electrical and Electronic Engineering, Xi'an Jiaotong-Liverpool University, No. 111 Ren'ai Road, Suzhou Industrial Park, Suzhou, P.R. China. His research interest focuses on power system security, integration of wind power into power grids, electric vehicle and energy internet.

Fei Xue was born in 1977 in Tonghua of Jilin province in China. He received his Bachelor and Master degrees in power system and its automation from Wuhan University in China in 1999 and 2002, respectively. He received the Ph.D. of Electrical Engineering degree from the Department of Electrical Engineering of Politecnico di Torino, Torino, Italy, 2009. He was the Deputy Chief Engineer of Beijing XJ Electric Co.,Ltd, Beijing, China and Lead Research Scientist in Siemens Eco-City Innovation Technologies (Tianjin) Co., Ltd, Tianjin, China. He is currently an associate professor



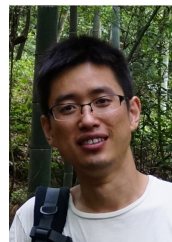
the University of Glamorgan, Wales, U.K., from 2005 to 2007, and joined the University of Liverpool in 2007. He is currently a Senior Lecturer with the Department of Electrical Engineering and Electronics, University of Liverpool. His current research interests include control and analysis of power system, smart grid, and renewable energy.

Lin Jiang received the B.Sc. and M.Sc. degrees in electrical engineering from the Huazhong University of Science and Technology, Wuhan, China, and the Ph.D. degree in electrical engineering from the University of Liverpool, Liverpool, U.K., in 1992, 1996, and 2001, respectively. He was a Post-Doctoral Research Assistant with the University of Liverpool from 2001 to 2003 and a Post-Doctoral Research Associate with the Department of Automatic Control and Systems Engineering, University of Sheffield, Sheffield, U.K., from 2003 to 2005. He was a Senior Lecturer with



power quality for railway traction systems.

Minwu Chen received the B.Eng. and Ph.D. degrees in electrical engineering from Southwest Jiaotong University, Chengdu, China, in 2004 and 2009, respectively. From 2010 to 2012, he undertook postdoctoral researches in the China Railway First Survey and Design Institute Group, Xi'an, China. Since 2018, he has been a Full Professor at the School of Electrical Engineering, Southwest Jiaotong University, Chengdu, China. From 2014 to 2015, he was a Visiting Scholar at the University of Birmingham, Birmingham, UK. His research interests include new technology and



Control.

Jie Yang was born in Anhui, China, 1979. He received the Ph.D. degree in the field of Rail Traffic Safety from then State Key Laboratory of Rail Traffic Control and Safety, Beijing Jiaotong University, China. He joined Jiangxi University of Science and Technology (JXUST) in 2005. He is now a professor, doctoral supervisor, the director of Jiangxi Key Laboratory of Maglev Technology (JKLMT) and the Institute of Permanent Maglev and Railway Technology (IPMRT) at JXUST. His research interests mainly focus on Permanent Maglev Trains and Energy-Efficient Train